scientific reports

Check for updates

OPEN

The role of prokaryotic mercury methylators and demethylators in Canadian Arctic thermokarst lakes

Nicola Gambardella[1,2], Joana Costa[1], Beatriz Malcata Martins[3], Diogo Folhas[3], Ana Patrícia Ribeiro[1,2], Holger Hintelmann[3,4], João Canário[3] & Catarina Magalhães[1,2]✉

Permafrost soils are critical reservoirs for mercury (Hg), with the thawing process leading to the release of this element into the environment, posing significant environmental risks. Of particular concern is the methylated form of mercury, monomethylmercury (MMHg), known for its adverse effects on Human health. Microbial communities play a pivotal role in the formation of MMHg by facilitating Hg methylation and in the demethylation of MMHg, slowing the crossing of toxic threshold concentration in the environment. However, the specific microbes involved still need to be understood. This study aimed to identify the microbial drivers behind changes in Hg speciation (MMHg and Hg) in permafrost thaw lakes and assess the significance of the biotic component in Hg biogeochemistry. Sediment samples from two thermokarst lakes in the Canadian sub-Arctic were collected during the winter and summer of 2022. Gene-centric metagenomics using whole-genome sequencing (WGS) was employed to identify key genes involved in mercury methylation (hgcA and hgcB) and demethylation (merA and merB), supported by qPCR analyses. A seasonal decline in microbial diversity, involved in the Hg methylation, and *hgcA* gene coverage was observed from winter to summer, mirroring patterns in mercury methylation rates. Notably, *hgcA* sequences were significantly more abundant than *merAB* sequences, with contrasting seasonal trends. These results indicate a seasonal shift in the microbial community, transitioning from a dominance of mercury methylation in winter to a predominance of mercury demethylation in summer. Environmental drivers of these dynamics were integrated into a conceptual model. This study provide new insights on the microbial processes influencing the Hg cycle in Arctic permafrost undergoing degradation.

The International Permafrost Association defines permafrost as ground (soil or rock and including ice or organic material) that remains at or below 0 °C for at least two consecutive years[1]. The surface soil layer on top of the permafrost thaws in summer and refreezes in winter, and it is defined as an active layer[2]). The present-day distribution of permafrost and ground ice is a combined effect of the historical development of permafrost during the glacial period and the present conditions of heat exchange at the Earth's surface and in the ground[3]. Permafrost thaw is critical evidence of the impact of climate change, particularly manifesting in Arctic regions where the warming effect is easily detectable[4]. Permafrost accounts for nearly half of all organic carbon stored within the planet's soil[5]. Permafrost thawing causes the organic matter present to become available for microbes that decompose and transform it, leading to the release of carbon dioxide and methane into the atmosphere[6]. The production of these greenhouse gases from the permafrost creates a positive feedback loop thereby amplifying the thawing process in a difficult-to-stop escalation. Additionally, the release of biological, chemical and radioactive materials that have been sequestered for tens to hundreds of thousands of years is also a concern[6]. Recent research shows that a warming climate that leads to the rapid thawing of permafrost has transformed the region from a carbon sink to a carbon source[7]. Regarding Hg stored in permafrost regions, it is estimated that Northern Hemisphere permafrost regions contain 1,656 ± 962 Gg Hg, of which 793 ± 461 Gg Hg is frozen in permafrost[2]. These values suggest that permafrost soils store nearly twice as much Hg as all other soils, the ocean, and the atmosphere combined[2]. The thawing causes the release of the previously stored

[1]Interdisciplinary Centre of Marine and Environmental Research (CIIMAR/CIMAR), University of Porto, Porto, Portugal. [2]Faculty of Sciences, University of Porto, Porto, Portugal. [3]Centro de Química Estrutural, Institute of Molecular Sciences and Department of Chemical Engineering, Instituto Superior Técnico, University of Lisbon, Lisbon, Portugal. [4]Water Quality Centre, Trent University, Peterborough, Canada. ✉email: catarina.magalhaes@fc.up.pt

Hg and consequently endangers the environment[8]. Mercury can affect human health by targeting the nervous system, heart, skin, lungs, liver, kidney, and reproductive system. Known exposure sources include vegetables from contaminated soils, and large predatory fish that are affected by the Hg flow starting from the permafrost thaw and ending in all major oceans throughout the Arctic Ocean[9]. The crippling and deadly effects of MMHg have been recognized globally since the severe Hg poisoning event in Minamata, Japan in 1956, after the release of Hg from a nearby industry[10]. Mercury is considered by WHO as one of the top ten chemicals or groups of chemicals of major public health concern[11]. It exists in various forms such as elemental, inorganic and organic, and these forms differ in their degree of toxicity.

Mercury is naturally present in environments and its biogeochemical cycle involves atmospheric transport, deposition to land and ocean, and re-volatilization[12]. Mercury is emitted to the atmosphere by both natural processes and human activities in its elemental form, Hg(0). Its oxidized form, Hg(II), is more soluble in water than Hg(0), and it consequently is the predominant form of mercury deposited to ecosystems through wet and dry deposition[12]. In this form, Hg has a much shorter lifetime in the atmosphere than Hg(0) (about days to weeks). Hg(0) conversion to Hg(II) happens in the atmosphere, from where it is brought to the terrestrial surface[12]. Microorganisms are known to methylate Hg(II) in mono-methyl mercury (MMHg) or demethylate MMHg in Hg(II) that could be subsequently reduced to Hg(0), leaving the oxidation of Hg(0) to Hg(II) to abiotic factors. Once on the surface, some of these microorganisms methylate Hg as a form of second metabolism, while others demethylate MMHg into Hg(II) as a form of detoxification mechanism[13]. Then, Hg returns to the atmosphere from soils by the reduction of Hg (II) to Hg(0) and subsequent diffusion or mass transport through soil and into the atmosphere[12]. Monomethylmercury produced by microorganisms bioaccumulates and biomagnifies through food webs (Fig. 1). For example, large predatory fish are more likely to have high levels of Hg as a result of eating smaller fish that have acquired Hg through ingestion of plankton.

The accurate identification of the microorganisms involved in the Hg methylation was maximized after Parks and colleagues[16] uncovered the genetic basis of this process in 2013, by identifying the presence of the genes *hgcA* and *hgcB* in Hg-methylators. Deletion of such genes was shown to abolish mercury methylation. The genes encode a putative corrinoid protein, *HgcA*, and a 2[4Fe-4 S] ferredoxin, *HgcB*, consistent with roles as a methyl carrier and an electron donor required for corrinoid cofactor reduction, respectively. These two genes have been shown to be present in all sequenced, confirmed methylators and absent in the sequenced, confirmed non methylators[16]. The native functions of *hgcA* and *hgcB* remain unknown, but these genes are known to be non essential for cell survival or proliferation[16]. The first phyla known to carry *hgcA*/*hgcB* gene clusters were *Proteobacteria*, *Firmicutes*, and *Euryarchaeota*. Additionally, in literature, Hg methylation has been associated with sulfate-reducing bacteria (SRB)[17], iron-reducing bacteria (FeRB)[18] and methanogenic archaea[19]. This was consequently reflected in the relationship between Hg methylation, sulfate-reduction, iron-reduction and methanogenesis[20]. More recent studies, who have applied cultivation-independent molecular methods, allowed the identification of *hgc* genes in microbial genomes from meta-omic data[21]. Nonetheless, there are still significant knowledge gaps in the identification of microorganisms capable of Hg methylation, largely because of the absence of *hgc* + cultured representatives from novel clades (i.e., outside the *Desulfobacterota*, *Firmicutes*, *Euryarchaeota*) with experimentally validated Hg-methylating capability[22]. The detection of *hgc* + MAGs is the common method to provide information about the taxonomic and metabolic characteristics of putative Hg

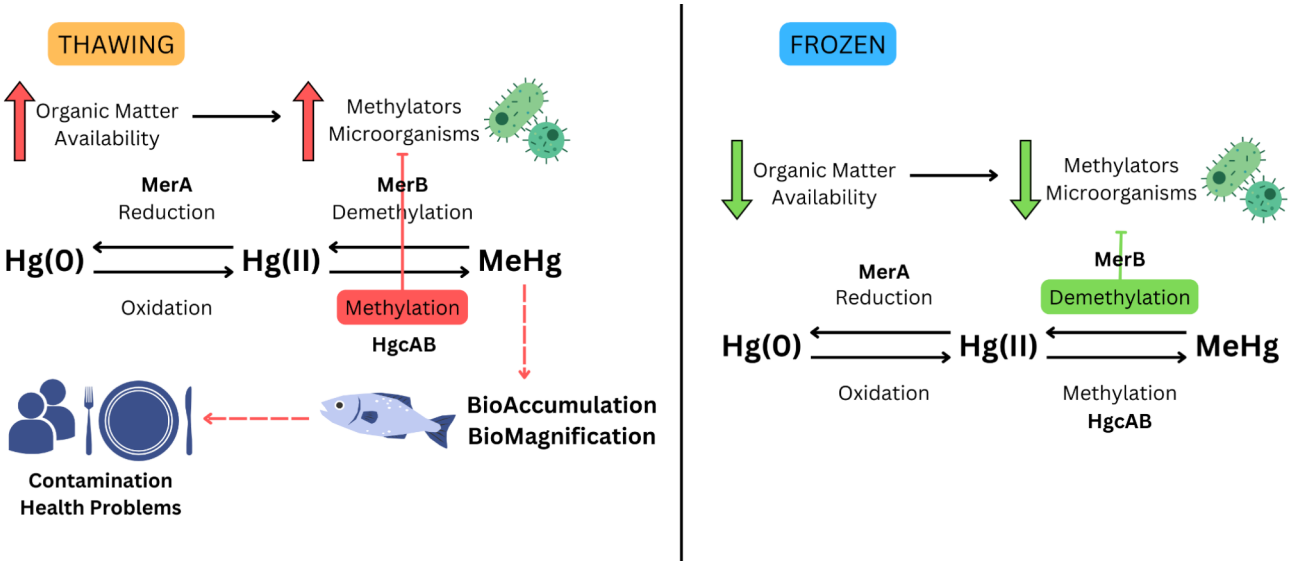

Fig. 1. Influence of permafrost thawing on Hg cycle. Permafrost thawing causes an increase in the availability of organic matter that consequently increases the population of methylators. This increase causes high production of MMHg that bioaccumulates in small fishes that are then eaten by large predatory fish causing mercury biomagnification. Such fishes are then consumed and mercury contamination may cause health problems[8,10,14,15].

methylators[23,24]. However, in some cases, microbial diversity is too high and/or the presence of Hg methylators is too rare to effectively identify them using such techniques[25]. In these cases, gene-centric metagenomic analyses and *hgc* metabarcoding are more effective. As previously stated, the current consensus attributes MMHg formation to anaerobic prokaryotes by a process that is specified by the "methylating genes", *hgcA* and *hgcB*. This is not the case for demethylation where multiple biotic and abiotic processes are documented to be involved and the exact mechanisms of some of the processes remain obscure[26]. The biotic processes are largely mediated by a prokaryotic Hg-resistance system: the mer operon. The mer system converts MMHg to CH_4 and Hg(0) when the activity of the organomercury lyase, MerB, is combined with that of the mercuric reductase, *merA*[26]. In literature, two main reactions are described: Oxidative Demethylation (OD) and Reductive Demethylation (RD). The first, OD, is favored in anoxic environments and low Hg concentrations, and the latter, RD, is favored in oxic and high Hg environments. Additionally, a study through incubation experiments with estuarine sediments by Compeau and Bartha[17] suggested that a demethylation process different from RD might exist. Currently, we still lack a complete understanding of which microorganisms are the primary drivers of Hg methylation and demethylation in diverse environments. In that sense, this study targeted the seasonal evaluation of the microbial communities involved in methylation and demethylation processes of different sediment layers of two thermokarst lakes, from the Canadian Subarctic. Here we apply molecular based and metagenomics approaches targeting different genes involved in these pathways and associated biogeochemical processes, such as sulfur reduction and methanogenesis. This research will advance our understanding of what microorganisms are related to the formation and decomposition of MMHg in permafrost thaw lakes and how they vary spatially and seasonally.

Results

Microbial communities decreased in taxonomic diversity at genus level in summer, when compared to winter season (Supplementary Fig. 3). Among the different microorganisms detected, several genera of Hg methylators belonging to the phyla *Chloroflexota*, *Methanomicrobia*, and *Desulfobacterota* were only identified in Winter. This seasonal shift on the prokaryotic community structure is more evident at genus level (Fig. 2). Globally, out of 50 genus, 18 genus were detected only in summer, and 12 only in winter. The most abundant microorganisms in both seasons belong to the genus *Pseudomonas*, *Bradyrhizobiom*, and *Polynucleobacter*. While the least abundant in both seasons are classified as *Streptomyces*, *Methylomonas* and *Rhodoferax*. Beta diversity analysis at genus level on the overall community resulted in a clear separation between seasons and lakes (Supplementary Fig. 4). No clear influence of the layer depth was detected (Supplementary Fig. 4).

HgcA gene sequences were obtained by using the marky-coco pipeline and the normalized *hgcA* gene coverage was used to investigate the presence of Hg methylators in the eDNA extracted from the sediments of the two thermokarst lakes, SAS1A and SAS2A. The methylation gene *hgcA* was found in all samples from the winter and summer campaigns (Fig. 3). This is in accordance with the PCR results that showed the presence of methylating communities in all samples when targeting both *hgcA* and *hgcB* genes using broad-range primers adequate for virtually all methylator clades (supplementary Fig. 1). Additionally, qPCR directed to *hgcA*, using clade-specific primers directed to *Desulfobacterota*, *Firmicutes* and methanogenic *Archaea*, also confirmed the presence of methylating communities belonging to these specific groups in the analysed samples (Fig. 4). Taken together, results showed that Hg methylating communities were present in both lakes and in both seasons, with *Desulfobacterota*, *Bacteroidetes*, *Chloroflexota* and *Euryarchaeota* being the main groups of methylators found (Fig. 3). Moreover, *hgcA* coverage values were lower in the summer in both lakes, when compared to winter (Fig. 3). Considering seasonal differences between the identified phyla, *Desulfobacterota* showed the most pronounced decrease from winter to summer; *Nitrospira* were only detected in the winter while *Fibrobacteres* were only seen in the summer. The summer-associated decrease in the relative percentage of *hgcA* + *Desulfobacterota* is consistent with qPCR results targeting *Desulfobacterota-hgcA* genes from the same samples (Fig. 4). Results from qPCR also showed an overall higher *hgcA* abundance in winter than in summer for the other analyzed clades, *Firmicutes* and methanogenic *Archaea* (Fig. 4).

Both SAS1A and SAS2A lakes showed a similar prokaryotic composition, in both seasons, when considering the top ten most abundant *hgcA* + phyla (Fig. 3). *HgcA* coverage fluctuated among the different depths in SAS1A lake, especially in the winter, while in SAS2A the cumulative value remained more stable (Fig. 3). The coverage of the marker genes involved in the final step of methanogenesis, *mcrA*, and in sulfate reduction, *dsrB*, exhibited the same profile of *HgcA* (Supplementary Fig. 5). Particularly, *mcrA* values were generally higher in winter than in summer, for the exception of the surface sediment layer (0–5 cm) in both lakes for which the values remain similar. The *dsrB* coverage showed a similar behaviour following the winter to summer transition with the exception of the surface sediment layer (0–5 cm) in lake SAS2A (Supplementary Fig. 5). These findings are corroborated by qPCR results on the potential higher abundance of hgcA + *Desulfobacterota*-clade (carrying *dsrB* gene), and hgcA + methanogenic archaea (carrying *mcrA* gene) in winter (Fig. 4). Correlation between *dsrB*, *mcrA*, and *hgcA* coverage resulted in a Pearson correlation coefficient of 0.8 and 0.87, for *dsrB-hgcA* and *mcrA-hgcA* respectively. Both correlations were statistically significant, with a p-value of 0.0009 and 0.0001, respectively (threshold fixed at 0.05).

MerA and *merB* genes, the main components of the prokaryotic defense mechanism against mercury, were successfully identified in the two lakes. Both spatial and seasonal differences were observed in the distribution of mer operon (Fig. 5). In fact, the two lakes presented different coverage between each other, with a tendency of higher coverage of *merA* and *merB* genes in summer (Fig. 5). The number of *merAB* sequences identified in our samples, intended as the overall number of genes sequences found at assembly level, were significantly lower than the number of *hgcA* + sequences.

Methylation rates exhibited seasonal variations, with generally higher values in winter than in summer (Fig. 6). Particularly, winter rates were higher than summer rates at 0–5 and 5–10 cm for SAS2A; at 5–10, and

Fig. 2. Prokaryotic taxonomy at genus level of lakes SAS1A and SAS2A in Summer and Winter (taxa below 0.5% of relative abundance was removed) calculated using Kaiju taxonomic assignments. Relative abundance was calculated from the percentage of metagenomic reads assigned to each taxon with a log10 transformation, considering the fraction of classified reads after Kaiju analysis. An asterisk (*) highlights microorganisms detected only in winter while hashtag (#) highlights the ones detected only in summer. *Methanobacterum*, *Methylocystis*, *Geobacter*, *Methanosarcina*, *Desulfosarcina* and *Desulfomonile*, highlighted in orange, are known Hg methylators detected only in the winter season in both lakes. The most abundant organisms belong to the genera *Pseudomonas*, *Bradyrhizobiom*, and *Polynucleobacter*.

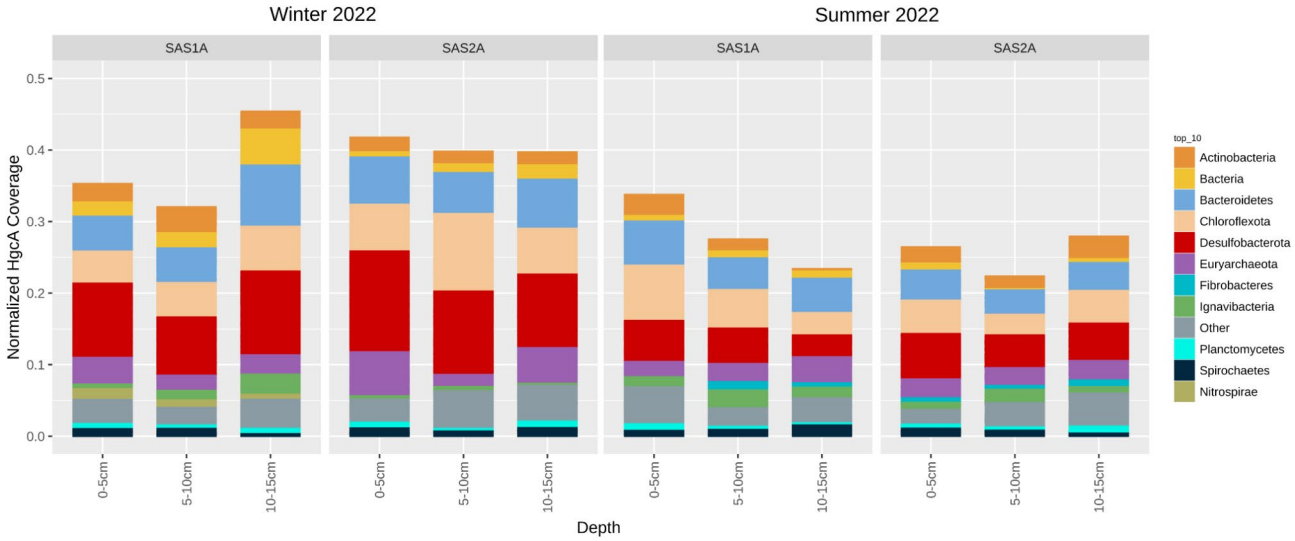

Fig. 3. Community structure at phylum level for *hgcA* positive prokaryotes. Normalized *hgcA* coverage for sediment samples in the two different lakes at different depths is shown. Results are divided between winter (left) and summer(right). Top 10 most abundant phyla are shown with different colors while other phyla are grouped together in the "Other" category (gray).

10–15 cm for SAS1A. On the contrary, the 0–5 cm layer in SAS1A and the 10–15 cm layer in SAS2A presented higher rates in summer. These findings align with the observed shifts in microbial communities involved in mercury methylation (Fig. 3) and demethylation (Fig. 5). Particularly, at 5–10 and 10–15 cm for SAS1A; at 0–5 and 5–10 cm for SAS2A. In SAS2A lake, *merA* coverage (Fig. 5) was following an opposite trend of the methylation rates (Fig. 6) and *hgcA* coverage (Fig. 3). Finally, the seasonal pattern shift found on the microbial communities involved in mercury transformations was consistent with a marked gradient of the environmental variables measured in the water in both seasons, with an impact on the entire lake system (Supplementary Table S3).

Discussion

The study of microorganisms involved in the Hg cycle in the permafrost regions, and the seasonal dynamics related to them are still poorly-known. In order to robustize these investigations, the application of multiple methodologies is advisable. In this study, we integrated molecular based methods (PCR and qPCR) with gene-centric metagenomics, anticipating that these approaches would complement each other and yield consistent results. The PCR and qPCR analysis verified the presence of methylating communities across all samples, demonstrating alignment with the coverage values obtained from gene-centric metagenomics. Notably, the latter approach identified *hgcA* sequences in instances where qPCR did not, such as in the summer SAS1A samples for both Archaea and Bacteria, and in SAS2A lake samples for Archaea alone (Fig. 3). This discrepancy is likely attributable to limitations associated with the primers employed, as these were directed to specific clades of methylators, with low abundances, thus probably below the method detection limit, or not present at all in these specific lakes. As is the case with all primer-based techniques, the choice of primers is critical for accurate target detection, and current *hgcA* primers are not yet fully optimized, with ongoing efforts to improve their design on an annual basis[27]. In contrast, metagenomic techniques that utilize shotgun sequencing do not rely on primers and are capable of revealing virtually all members of the methylating community. Despite these differences, the findings demonstrated successful amplification of *hgcA* genes via PCR and qPCR and effective retrieval of these genes from the metagenomic dataset using gene-centric metagenomics.

Conducting research in Arctic environments presents logistical challenges, our sampling reached the maximum depth permitted by the available equipment, due to the presence of frozen soil at lake bottoms during winter. However, sampling deeper layers might have provided additional insights into Hg methylation processes. Recent studies have demonstrated that anoxic conditions persist year-round at the sampled depths and even at greater depths than those examined in this study[28]. Moreover, from our results, there is no evidence to suggest that either methylation rates or mercury-related microbial activity increase with depth (Fig. 6). The study's sample size presents certain limitations, as only one sample was collected per depth, with three depths analyzed in total across two lakes during two different seasons. While this design provides a preliminary understanding of spatial and temporal variations, the limited number of samples may restrict the generalizability of the findings and the ability to capture fine-scale heterogeneity within the ecosystems. Interestingly, despite the limited sample size, our analysis successfully revealed both spatial (Supplementary Fig. 3) and temporal variations (Supplementary Figs. 2 and 3, Figs. 4, 5, and 6) within the microbial communities inhabiting these lakes.

The lakes studied (SAS1A and SAS2A) are representative of the broader thermokarst lake environment, as they share key ecological and environmental characteristics observed in other thermokarst lakes across the subarctic and Arctic regions. Several studies have documented the ecological significance of thermokarst lakes

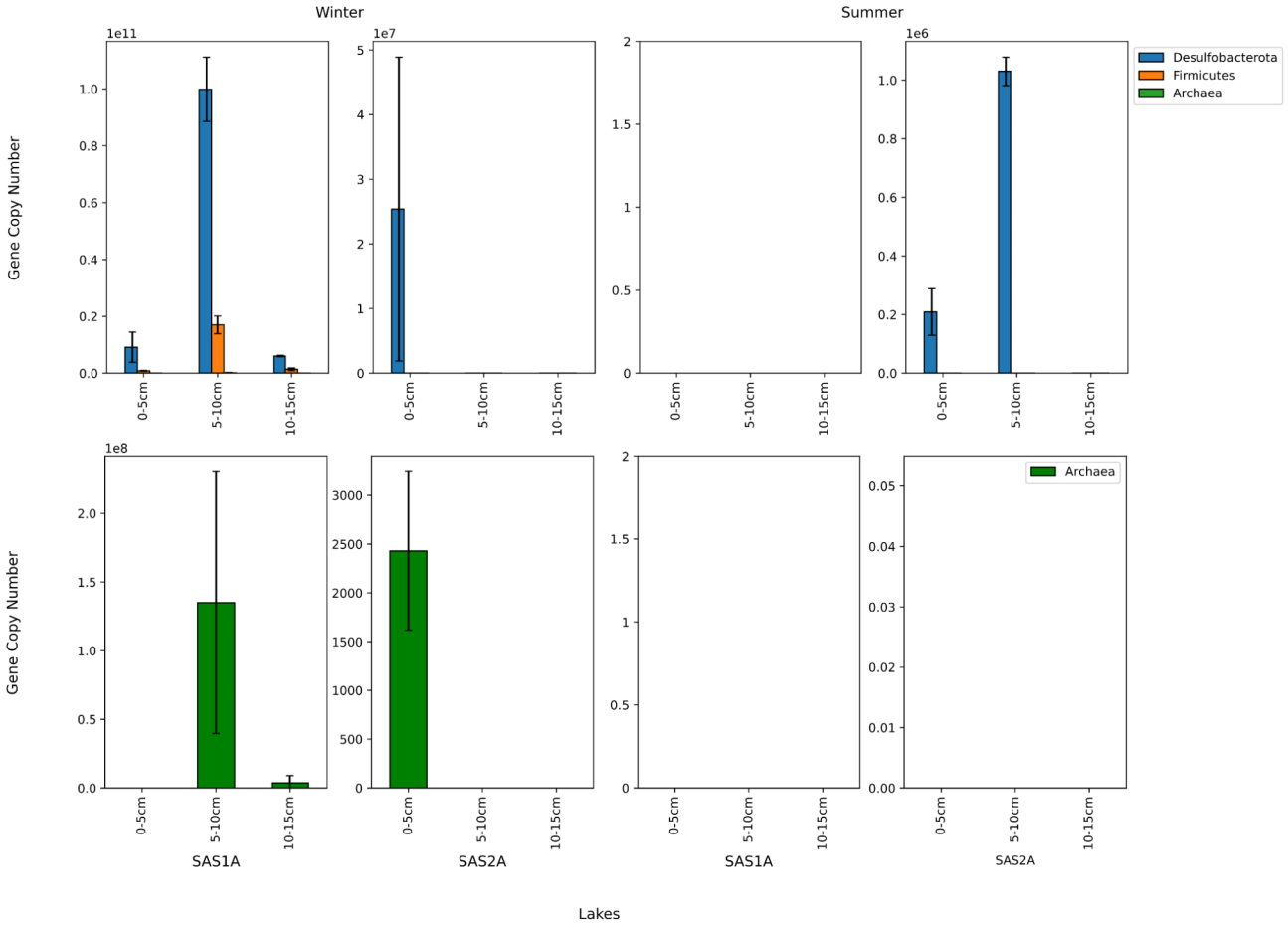

Fig. 4. Estimated *hgcA* abundance as mean gene copy number per gram of sediment ± standard error ($N = 2$), obtained by qPCR analysis of extracted eDNA samples, using clade-specific primers directed to *Desulfobacterota* (blue), *Firmicutes* (orange) and *Archaea* (green). Different y-axis scales are presented as the values are in different order of magnitude. Such magnitude is indicated on the left top corner of every subplot (if present).

in these areas, and the characteristics of the SAS1A and SAS2A lakes (Supplementary Table S3) align with the findings from these broader investigations[29–33]. In fact, we believe the lakes investigated in this study provide a valuable model for understanding the complex interactions between climate change, microbial processes, and Hg cycling in similar ecosystems across the Arctic and subarctic regions.

Our findings answer the necessity to explore the diversity of both Hg methylators and MMHg demethylators in the Arctic permafrost thaw lakes. At the present, few studies have covered Hg methylation in areas with thawing permafrost[34]. Thermokarst wetlands, ponds and lakes have been repeatedly identified as Hg methylation hotspots across the Arctic due to the concurrent mobilization of carbon and nutrients, creating conditions suitable for methylation[34,35]. This observation is confirmed by our results as both physicochemical and microbial data point to SAS1A and SAS2A as a Hg methylation hotspot (Figs. 3 and 6). The decrease in the Hg microbial players observed from winter to summer argues against the present knowledge where the usual observed trend is an increase in the abundance of methylators due to the thawing process of Arctic ecosystems[36] (Fig. 1). However, since the variation and concentrations of total Hg (THg), inorganic mercury (IHg), and MMHg in different climate zones may exhibit different trends[37] we hypothesize that the studied region possesses a particular Hg cycle system and dynamic. The seasonal-specificity of some genera observed in our soil samples shows the adaptability of the community to the different environmental conditions and may be the key to understanding how this kind of environment acts in response to climate change.

The normalized coverage of *hgcA* genes showed that methylator organisms presence is greater in winter than in summer and that their increase is linked to higher methylation rates in the soil samples (Figs. 3 and 6). Number of *hgcA* + sequences, significantly higher than the number of *merAB* sequences, suggest a prevalence of Hg methylators in the environment. Our results showed that prokaryotic genera identified only in winter and known to be involved in the Hg cycle were *Methanobacterium*, *Methylocystis*, *Geobacter*, *Methanosarcina*, *Desulfomonile* and *Desulfosarcina*[21,22,38–41] (see Fig. 2). Among the ones found only in summer, there were some genera with Hg cycle involvement, namely, *Sphingomonas*, *Frondihabitans* which were already identified to possess *merA* genes, *Rhodoplanes*, *Methylotenera* which *merA* presence was assessed and tested for bioremediation[42],

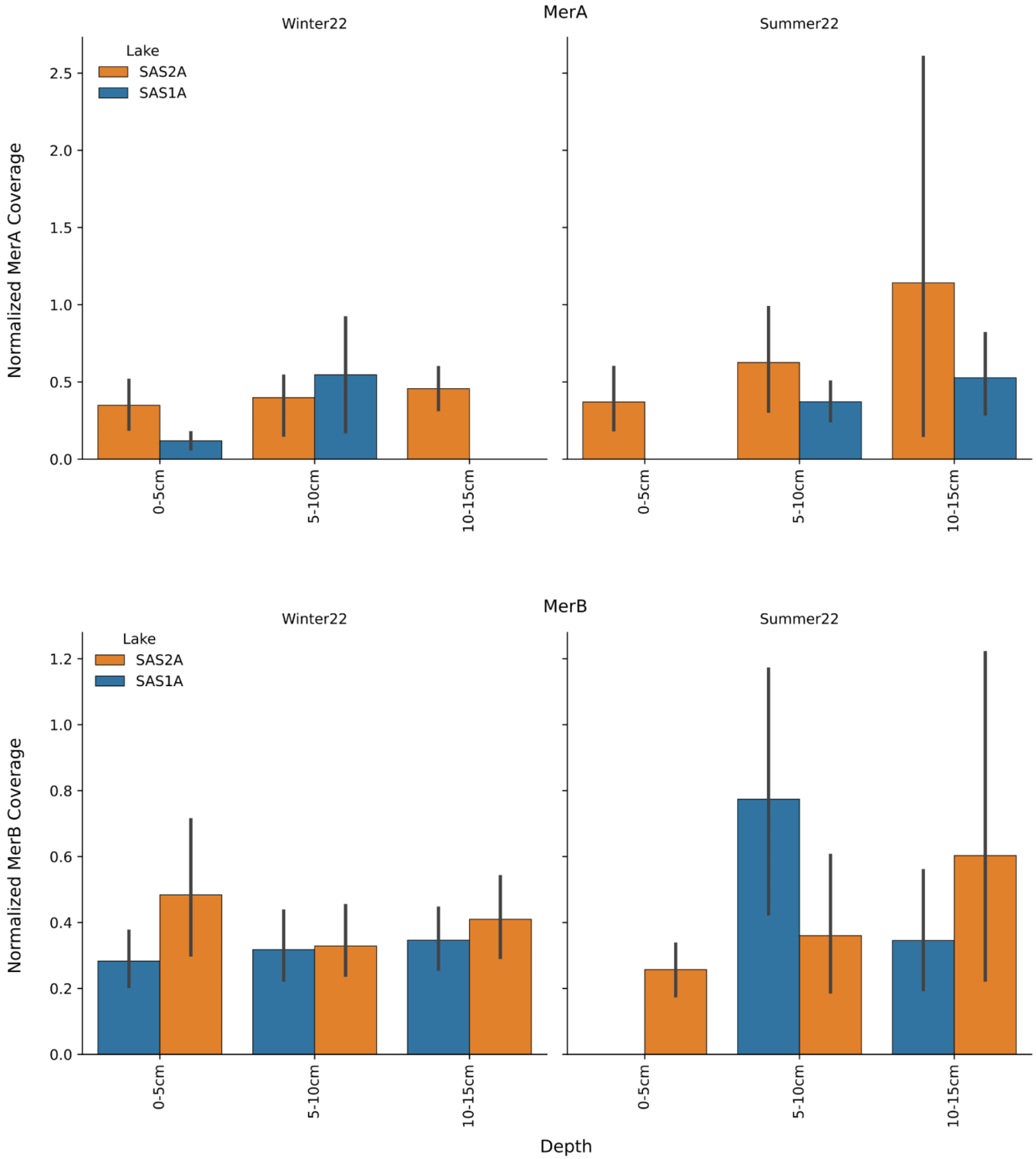

Fig. 5. Coverage of *merA* (top panel) and *merB* (bottom panel) genes during summer (left panel) and winter (right panel) 2022 in SAS1A (orange) and SAS2A (blue) lakes. The coverage was calculated and normalized based on the *merA* and *merB* gene sequences identified in the metagenomic data.

and *Mesorhizobium* already known in the literature for *merA* gene present[43]. *Granulicella* and *Variovarax* were also identified, though their roles in the Hg cycle remain uncertain (see Fig. 2)[44–50]. These results suggest that microbial communities and in particular *Methanobacterium*, *Methylocystis*, *Geobacter*, *Methanosarcina*, *Desulfomonile* and *Desulfosarcina* play an important role in the availability of MMHg in these thermokarst lakes. Genera identified exclusively during the winter season, coinciding with a peak in *hgcA* gene coverage, include well-established sulfate-reducing bacteria (SRB) and methanogens that have been previously associated with Hg methylation activity[22,39–41]. This study observed an increase in genes related to sulfate reduction (*dsrB*) and methanogenesis (*mcrA*), which appeared to correlate with *hgcA* coverage (Supplementary Fig. 6). These findings

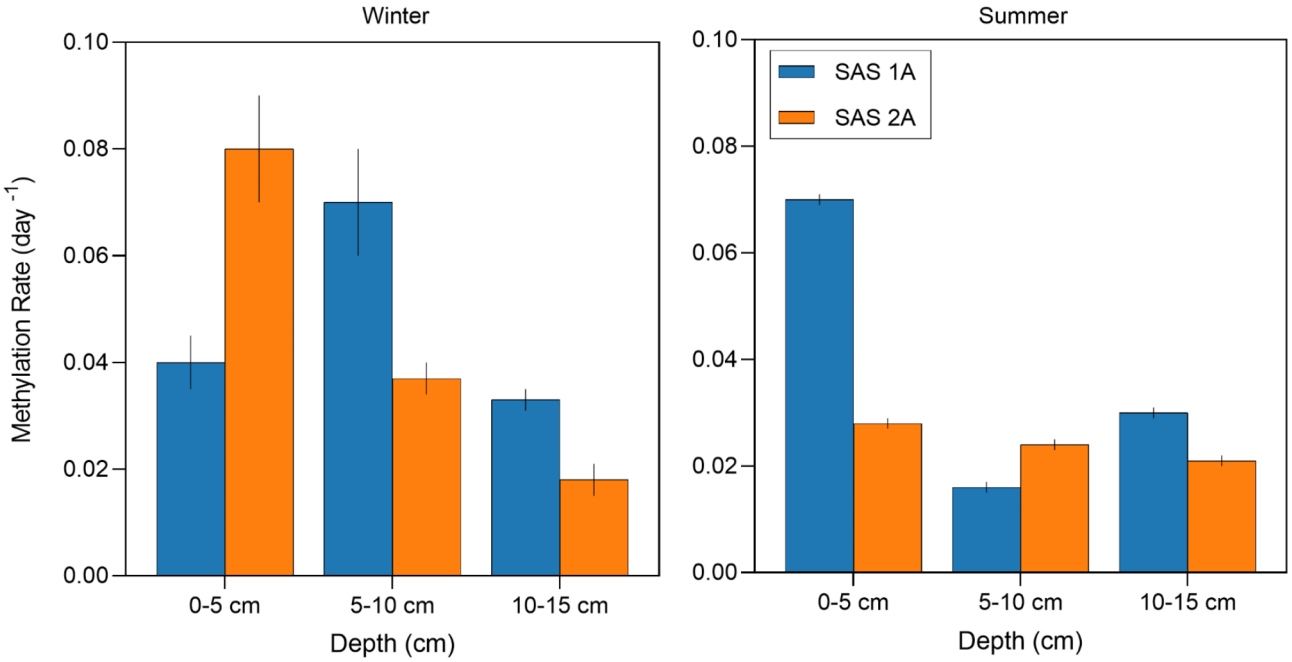

Fig. 6. Methylation rates of Hg depicted across the three distinct sediment's depths within the two lakes under investigation (SAS1A and SAS2A) during both winter and summer seasons. Values are expressed as day $^{-1}$ and triplicates of MM^{200}Hg and ^{200}Hg were measured to assess the measurement precision. The error in methylation rates was calculated using the uncertainty propagation formula.

align with existing literature, further supporting the critical roles of sulfate reduction and methanogenesis in Hg methylation. The observed changes in the mercury-related microbial community have been associated with variations in Hg methylation rates. This relationship can be explained by the fact that an increase or decrease in *hgcA* gene coverage corresponds with a respectively higher or lower capacity within the community to methylate Hg. In addition, the metagenomic data on *merA* and *merB* corroborated the *hgcA* metagenomic data, indicating that the observed decrease in *hgcA* coverage and methylation rates during summer coincided with an increase in the coverage of *merA* and *merB*. These results suggest a shift in the microbial community from a predominance of mercury methylation in winter to a prevalence of mercury demethylation in summer. However, due to the technical difficulties of *merA* and *merB* identification, the possible demethylation potential of the community may be underestimated, as the cut-off necessary for confidently identifying such genes excluded more than 80% of the sequences. It is also important to note that causality cannot be inferred from this experimental design alone. Future studies should focus on the *hgcAB*, *merAB* genes, and methylation rates in controlled laboratory settings to establish causality. Additionally, metatranscriptomic approaches could be employed in future research to assess the actual gene expression related to these processes.

An increase in oxygen levels from winter to summer was observed in the water column of both lakes (Supplementary Table S3), which would be consistent with a brief enhancement of oxygenation at the surface-water interface at SAS1A. However, sediments remained anoxic throughout both seasons[28]. These anoxic conditions are conducive to the reductive dissolution of iron, sulfate reduction, and anaerobic organic matter consumption via methanogenesis[53].

The increased presence of dissolved organic carbon (DOC) and reduced sulfur (in the form of S^{2-}) observed in winter compared to summer (Supplementary Table S3) aligns with the theoretical concept of enhanced Hg bioavailability. Previous studies have demonstrated that both DOC and sulfur compounds have the capacity to bind to Hg, thereby promoting its methylation[54]. This has been documented in several studies that underscore the role of DOC and sulfur in facilitating Hg methylation processes[54,55].

The fluctuations in *mcrA* coverage, which strongly correlate with *hgcA* values, further reinforce the established link between Hg methylation and methanogenesis, as reported in previous studies[19,20]. *mcrA* is a gene encoding the alpha subunit of Methyl-coenzyme M reductase (MCR), an archaeal enzyme responsible for catalyzing the final step in methanogenesis and the initial step in anaerobic methane oxidation[56]. Thus, *mcrA* serves as an indicator of methanogenic potential. Additionally, *dsrB*, another important marker gene, displayed similar trends, with its coverage positively correlating with *hgcA*. *DsrB* is part of the dissimilatory sulfite reductase (DSR) pathway, which catalyzes the final step of sulfate reduction to sulfide[57]. Specifically, *dsrB* expresses the beta subunit of DSR, and thus serves as an indicator of sulfate reduction potential. Overall, the variation in the coverage of genes involved in mercury methylation, sulfate reduction, and methanogenesis is consistent with the anoxic conditions observed at the sediment level of the studied lakes.

The integration of environmental data (Supplementary Table S3) with microbial community analyses suggests a seasonal dynamic influencing Hg methylation and demethylation processes. During winter, elevated levels of

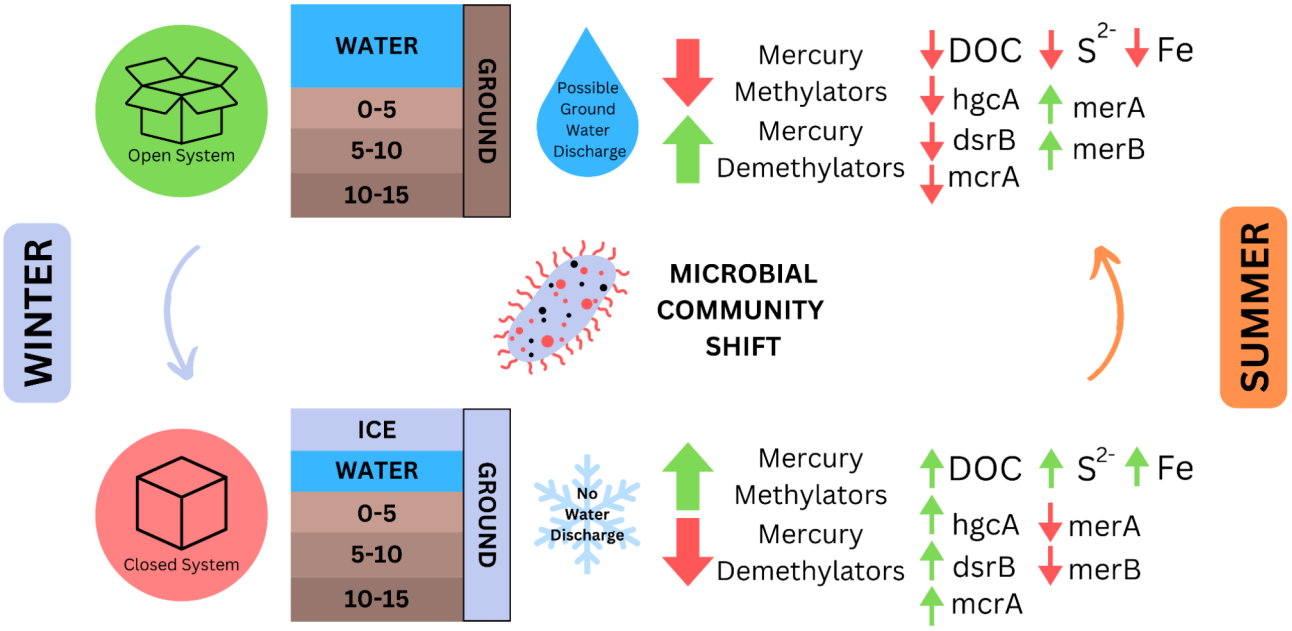

Fig. 7. Conceptual model of internal dynamics of thermokarst lakes (sediment layer depth in cm). Seasonal environmental dynamics and microbial community shifts in thermokarst lakes. During winter, ice covers these lakes, isolating the water column and sediments from external inputs and restricting oxygen exchange, resulting in rapid oxygen depletion. The concentration of DOC increases due to reduced liquid water volume, while reduced sulfur (S^{2-}) and Fe(II) concentrations decline from winter to summer. Microbial community composition in sediment layers across three depths shifts in response to seasonal environmental changes, displaying opposing profiles of potential Hg methylation and demethylation. Genes associated with sulfate reduction (*dsrB*) and methanogenesis (*mcrA*) show seasonal patterns consistent with variations in hgcA gene coverage, indicating their link to Hg methylation processes.

DOC and reduced sulfur species (S^{2-}) might enhance mercury bioavailability, promoting MMHg formation[54]. This process is supported by the increased presence of microbial Hg methylators, as evidenced by the higher coverage of hgcA (Fig. 3). In contrast, summer conditions exhibit reduced levels of DOC and S^{2-}, leading to decreased Hg bioavailability[54]. During this period, the existing MMHg is subject to demethylation by microbial Hg demethylators. This shift is reflected in the microbial community composition, with a lower coverage of *hgcA* and increased coverage of *merA* (Figs. 3 and 5). We also hypothesize that the increase of Fe(II), measured in the winter season, may be a possible micronutrient source that may activate Hg methylators, contributing to the community shift (Fig. 7), as previous study has proven a promoting effect of this element on MMHg production[58]. However, further studies are required to clearly define its relation, as the inhibitory effect of this element has been proven in the literature[59]. Additionally, the unfreezing process affecting the ground may favor underground water discharge processes that enhance possible exchanges between the lakes and the surrounding environment[60]. DOC is diluted in the whole water liquid volume and iron levels are high (Fig. 7). Additionally, during summer the high temperature and light exposure may cause the photodegradation of MMHg contributing to the observed low concentration of such a compound[61]. In fact, redox transformations between the ionic and elemental Hg forms affect MMHg production by controlling the amount of substrate that is available for methylation[62]. Arctic lakes were previously reported to be exposed to 24 h of daylight, resulting in substantial UV exposure to the lake ecosystem[36]. However, the photodegradation effect is attenuated in SAS1A and SAS2A by the high amount of particles in the water (Supplementary Table S3). During winter, the thermokarst lakes get covered by a layer of ice that shields the water and the sediments below from external inputs. Such an ice cover stops the exchange of oxygen that is rapidly consumed in the water column, transforming the lake into an anoxic environment[15]. DOC concentration, before diluted in a larger volume, increases due to the decrease of volume of liquid water. The sediment layers (studied at three different depths) experience a shift in the microbial communities due to the change of such environmental conditions. It is widely accepted that MMHg is mainly produced by anaerobic microorganisms in the environment and its production rate is therefore related to their presence and activities[63]. The increase in DOC concentration is well-explained by the decrease of the liquid water in winter. However, such increase may also be associated with the transport of MMHg and Hg methylation. Alternatively, it might be an indirect indicator of higher biological activity, potentially driving an increase in MMHg production[36]. Another environmental variable to consider in the Hg dynamic is the groundwater discharge, especially considering that the investigated lakes are located approximately 500 m from a river (Supplementary Fig. 2). The authors are currently investigating this possibility in ongoing studies to assess the potential movement of Hg to and from the river.

Interpreting environmental factors in relationship with microbial communities is complex due to several possible confounding factors. In addition to the ones measured in this study, other unmeasured environmental values might also play significant roles. The proximity of the lakes to a river introduces the potential for hydrological exchanges that could transport Hg and alter DOC concentrations. Moreover, mentioned seasonal light exposure and potential UV-driven photodegradation of MMHg might vary due to lake turbidity and particle content, potentially skewing the seasonal methylation and demethylation balance[61]. The speciation of mercury (e.g., inorganic Hg^{2+}, elemental Hg^0, and methylmercury MMHg) can greatly influence its bioavailability and microbial uptake[20,37]. Variations in speciation due to changes in redox conditions, DOC binding, or sulfur interactions might confound the link between microbial activity and Hg methylation or demethylation rates. Another important factor to take in account is the composition of DOC, which directly impacts Hg bioavailability[58]. From a biological perspective, the observed balance between *hgcA* and *merA* gene coverage may be influenced by complex microbial interactions not captured in this study. Addressing these confounding factors in future research will surely strengthen the reliability and interpretability of the results.

Our study offers new insights into the microbial contribution to the Hg cycle in the Arctic and reinforces the connection between environmental physicochemical characteristics and microbial methylation capabilities[17,20]. Regarding microbial diversity in the SAS lakes, our findings indicate a complex and diverse community, as evidenced by taxonomic classification results (see Figs. 2 and 3). We hypothesize a conceptual model of the dynamic of these lakes (see Fig. 7) consistent with the measured environmental parameters and general Hg dynamic in the Arctic[8]. Winter conditions were associated with higher *hgcA* gene abundance, suggesting an increased potential for mercury methylation under anoxic conditions enriched with DOC and sulfur. In contrast, summer conditions exhibited lower *hgcA* coverage, and higher coverage of *merA* gene, which may be linked to an increase of Hg demethylation over mercury methylation. This seasonal shift was reflected in the lower levels of MMHg in summer (Supplementary table S6) and methylation rates (Fig. 6, Supplementary table S4), indicating a dynamic interplay between environmental factors and microbial activities.

The unique characteristics of thermokarst lakes require further study due to their dynamic nature. The microbial communities in these environments experience significant environmental stress, as demonstrated by changes observed in the overall community (Fig. 2) and specifically in Hg methylation and demethylation processes (Figs. 3 and 5, respectively). We demonstrated that the thermokarst lakes analyzed possess the metabolic capability for Hg methylation and demethylation, and that such capability varies seasonally. The results from non PCR-based methods were confirmed by PCR and qPCR, able to detect *hgcAB* (Supplementary Fig. 1) and *hgcA* genes (Fig. 4), respectively, clearly demonstrating their presence in both thermokarst lakes. These results are improving our understanding of the Hg-cycle pathways and its prokaryotic communities, poorly-known in permafrost areas. This and future research are important to evaluate the hazards caused by the permafrost thawing, and its impacts on Arctic ecology, ecosystem services and human health. Future works may rely on metatranscriptomics analysis to quantify the expression of the genes involved in the Hg cycle.

Methods

Study area and sample collection

The fieldwork was conducted in thermokarst lakes on a sporadic permafrost zone located in Sasapimakwananisikw (SAS) River Valley (55°13'N;77°42'W), near the communities of Whapmagoostui-Kuujjuarapik, Nunavik (Quebec), Canada. SAS thermokarst lakes originate from the thawing of palsas - peaty permafrost mounds containing a core of alternating layers of segregated ice and peat. Such structures are formed due to the water freezing during winter, forcing the soil upwards; they tend to exhibit significant organic matter content due to the presence of peat[14]. Two thermokarst lakes were sampled in winter and summer of 2022. In lake SAS 1 A (55°13'07.7 N, 77°42'28.4 W) and lake SAS 2 A (55°13'35.6 N, 77°41'49.1 W) sediment samples were collected at 3 different depths that ranged between 0 and 15 cm. Sediment depth was limited by the available equipment, and in particular by the frozen ground during the winter sampling. Both seasonal sampling campaigns followed a protocol for collecting sediment eDNA for DNA extraction that consisted of: extraction of a sediment core in the field, transport to the laboratory, division of the core in three parts (0–5, 5–10, and 10–15 cm), collect of soil using a sterile tip of 5 ml avoiding stones, storing samples by freezing them at -80 °C. Protocol is available also at https://www.protocols.io/blind/70FE3129D34E11EE8AEF0A58A9FEAC02.

To determine the methylation rates at each depth, incubation experiments were conducted using isotope enriched Hg. A target mass of 1.25 ng $^{200}Hg(II)$ was added to approximately 10 g of wet sediment to to track the formation of $MM^{200}Hg$.

Total mercury analysis

Total mercury analysis in sediments followed a procedure adapted from the EPA method 1631[65]. Approximately 200 mg of dry sample was weighed and spiked with ^{199}Hg as the internal standard. The samples were digested with 5 mL of a 7:3 HNO_3/H_2SO_4 acid mixture and left overnight on a hot plate at 110 °C. The digests were then diluted to 25 mL with Milli-Q® water. Each batch of samples included reference materials (PACS-2 and IAEA-475) and digestion blanks to ensure accuracy.

Mercury isotope concentrations were quantified using a continuous-flow cold-vapor system coupled to a QQQ ICP-MS (Agilent® 8800). In the cold-vapor system, the sample was continuously mixed with a solution of 3% (w/v) stannous chloride in 10% HCl (v/v), reducing Hg to its elemental form, which was then introduced in the plasma of the ICP-MS. The concentration of Hg isotopes was calculated as described in Hintelmann and Ogrinc[66]. The values and standard deviation of the calculated total Hg concentrations are shown in Supplementary Table S5.

Methylmercury analysis

Methylmercury analysis in sediments followed a procedure adapted from the EPA method 1630[67]. Approximately 200 mg of dry sample was weighed into Teflon vials to which was added 10 mL of Milli-Q® water and $MM^{199}Hg$ as an internal standard. Afterward, it was added 500 µL of H_2SO_4 (9 M) and 200 µL of KCl (2 M) and the vial was placed in a heating block at 140℃. Methylmercury was distilled into a receiving vial with 5 mL of Milli-Q® water, under a constant N_2 flow (60 mL min^{-1}). Each batch of samples included reference materials (MESS-4, BCR-580 and IAEA-475) and distillation blanks to ensure accuracy. Methylmercury isotope concentrations were quantified using gas chromatography coupled with an ICP-MS (GC/ICP-MS), following the methods described by Hintelmann and Evans[69] and Hintelmann and Ogrinc[66]. Specifically, a Tekran 2700 system was coupled to a QQQ ICP-MS (Agilent® 8800) for this purpose.The values and standard deviation of the calculated total mercury concentrations are shown in Supplementary: Table S6.

Methylation rates

The concentrations of $^{200}Hg(II)$ and $MM^{200}Hg$ were calculated as described in Hintelmann et & Ogrinc[66]. The methylation rates (expressed in day^{-1}) were calculated assuming a first-order kinetics[68], as shown in the following equation.

$$K_m - [MM^{200}Hg]_{t=24h} / \left(\left[{}^{200}Hg(II) \right]_{t=0h} \times t \right)$$

where $[MM^{200}Hg]_{t=24\ h}$ is the concentration of $MM^{200}Hg$ after 24 h, $[^{200}Hg(II)]_{t=0\ h}$ is the concentration of added $^{200}Hg(II)$ in the samples and t is the time of incubation. Analysis of triplicates was conducted to measure precision. The values and standard deviation of the calculated methylation rates are shown in Supplementary: Table S4.

DNA extraction and quantification

The samples were defrosted, at room temperature, and the eDNA was extracted using DNeasy® PowerSoil® Pro Kit, according to the manufacturer's protocol (Sample to Insight DNeasy ® PowerSoil ® Pro Kit Handbook, 2021), from 250 mg of soil. Purified eDNA was stored at − 80 °C until further use. The eDNA concentration of each sample was measured using the Qubit method, according to the manufacturer's instructions.

PCR and sequencing

Identification of hgcAB by PCR

Identification of *hgcAB* sequences by PCR was performed in eDNA extracted from sediment samples and from *Geobacter sulfurreducens* (DSMZ 12127) as positive control, according to the methodology described by Christiansen et al.[70] and modified by Gionfriddo et al.[27], with some adaptations. Briefly, for *hgcAB* amplification, 20µL reaction mixture consisting of 2 µM ORNL-HgcAB-uni-F and ONRL - HgcAB-uni-32R primers, 10 µL of My Taq Mix (containing My Taq DNA Polymerase - Meridian Bioscience) and 100 pg to 10 ng of eDNA was runned in Veriti™ 96-Well Thermal Cycler. A touch-down PCR protocol was used according to Gionfriddo et al.[27] (Supplementary Table S2). The amplified fragments were visualized under UV light, after electrophoresis in a 2% in TAE-buffer agarose gel, stained with SYBR Safe (Gel stain -ThermoFisher Scientific).

Identification of hgcA genes in different bacterial clades by qPCR

For the identification and quantification of *hgcA* in different prokaryotic clades, we used clade-specific *hgcA* directed primers and *q*PCR protocols[70]. Specifically, primers directed to the groups *Desulfobacterot*a (former Deltaproteobacteria), *Firmicutes* and Archaea were used. The primers and amplification protocols used for each clade are described in Supplementary Tables S1 and S2.

Optimal primers concentrations for the qPCR were determined (Supplementary Table S1) for each reaction after evaluation of the highest fluorescence signal at lower Ct number. Reactions were performed on the Step One Plus Real Time PCR System (Applied Biosystems) using 10 µl of Power SYBR® Green PCR Master Mix (Alfagene), 2 µl of template eDNA (20-24ng), 2 µl of each primer, in a total volume of 20 µl per reaction. All samples were ran in duplicate, and no template control (NTC) reactions were performed to ensure the non-formation of primers dimers and/or unspecific products during the amplification process. Standard curves were generated for *hgcA*, using eDNA extracted from different microorganisms, used as positive controls for each of the clade specific primer pairs (as described in Supplementary Tables S1 and S2). Quantification results of *hgcA* in each sample are shown as gene copy number, calculated according to the following expression:

$$Gene\ copy\ number/g\ of\ sediment = \left(\frac{\left(10^{\left(\frac{Ct - Yinter}{Efficiency} \right)} \times Avogadro\ constant \right)}{Amplicon\ length \times 10^9 \times 660} \right) / g\ of\ sediment$$

Where, Ct equals the threshold of each amplified sample, Yinter equals the intersection of the standard curve in the y-axis and efficiency is obtained from the standard curve generated.

Sequencing

Samples were sequenced by BGI company (Shenzhen, China) using DBNseq™ technology. This method uses peculiar DNA nanoballs (DNBs) generated by rolling circle amplification (RCA) of the DNA fragments that, placed onto a patterned array chip, are sequenced. Laser excitation and imaging capture the incorporation of fluorescently labeled nucleotides whose signal is converted into DNA sequence data. This technology has been proven to be comparable to Illumina for whole genome analysis[71].

The sequencing outputs presented an average of 71,966,315 sequencing reads, each comprising 150 nucleotides. These reads exhibited a mean quality score of 35 and an average coverage of 10,7 Gbp per sample.

Bioinformatic analysis

The detection, counting and taxonomic identification of *hgcAB* genes was done with marky-coco[21]. The metagenomes were trimmed and cleaned using fastp[72] with following parameters: -q 30 -l 25 --detect_adapter_for_pe --trim_poly_g --trim_poly_x. A de novo single assembly approach was applied using the assembler megahit 1.1.2[73] with default settings. The annotation of the contigs for prokaryotic protein-coding gene prediction was done with the software prodigal 2.6.3[74]). The DNA reads were mapped against the contigs with bowtie2[75], and the resulting .sam files were converted to .bam files using samtools 1.9[76]. The .bam files and the prodigal output .gff file were used to estimate read counts by using featureCounts[77]. In order to detect hgc homologs, HMM profiles derived from the Hg-MATE.db.v1 were applied to the amino acid FASTA file generated from each assembly with the function hmmsearch from hmmer 3.2.1[78]. The reference package '*hgcA*' from Hg-MATE.db.v1 was used for phylogenetic analysis of the *hgcA* amino acid sequences. Briefly, amino acid sequences from gene identified as *hgcA* gene homolog were (i) compiled in a FASTA file, (ii) aligned to Stockholm formatted alignment of *hgcA* sequences from the reference package with the function hmmalign from hmmer 3.2.1 (iii) placed onto the *hgcA* reference tree with the function pplacer and (iv) classified using the functions rppr and guppy_classify from the program pplacer[79].

The resulting output was further analyzed in RStudio[80] (RStudio Team, 2020) where true detection of *hgcA*, *hgcB*, *merA* and *merB* followed the indication given by Capo and colleagues[21]. Specifically, the presence of one of the following motif was assured to define a detected *hgcA* gene sequence as true match: "NVWCAAGK", "NVWCASGK", "NVWCAGGK", "NIWCAAGK", "NIWCAGGK" or "NVWCSAGK". True match for HgcB gene was defined by assessing the co-localization of the putative gene sequence with *hgcA* sequence and the presence of one of the following motifs: "CMECGA", "CIECGA". Gene coverage was normalized using rpoB gene coverage and the taxonomy was assigned using NCBI taxonomy.

Community structure was investigated at read level using Kaiju[81]. Relative abundance was calculated from the percentage of reads assigned to each taxon, considering the fraction of classified reads after Kaiju analysis. Biodiversity indexes, such as alpha and beta diversities, were calculated using the Python libraries scikit-bio (https://scikit.bio) and scipy (https://scipy.org). In particular, alpha diversity has been calculated using Shannon index. Beta diversity has been calculated using Bray-Curtis dissimilarity and clustered using single linkage, namely the Nearest Point algorithm to produce a dendrogram where each cluster is composed by drawing a U-shaped link between a non-singleton cluster and its children.

MerAB identification was obtained through a combination of marky-coco pipeline[21] and an ad-hoc processing developed by the authors. Within the marky-coco pipeline, metagenomic reads were aligned using hmmsearch with hidden markov models (HMM) based on a *merAB* database obtained from Christakis et al.[82]. The resulting *merAB* putative sequences were then aligned to two established references, *merA* of *Bacillus sp.* RC607 (NCBI accession number: BAB62433) and MerB of *Escherichia coli* plasmid R831b (Uniprot accession number P77072) using muscle[83]. The alignment allowed setting each sequence a score based on the presence of conserved amino acids known in the literature for their essential role in the enzymatic activity of the protein. The score was used as threshold and resulting sequences were defined as high-confidence *merAB* sequences and used in our results. Gene information was then interpreted in relationship with depth and geographical distribution of the sample.

mcrA identification was based on the reference database provided in Yang et al.[84] (available at https://doi.org/10.5880/GFZ.4.5.2014.001). The reference sequences were aligned using muscle and the alignment was used to create a hidden-markov model (hmm) with hmmbuild function from hmmer 3.2.1[78]. Gene prediction was performed at assembly level using prodigal 2.6.3[74] and parsed for matches using the built hmm model.

dsrB identification was based on the reference database provided in Diao et al.[85] (available at https://www.arb-silva.de/projects/dsrabsilva/). The reference sequences were aligned using muscle and the alignment was used to create a hidden-markov model (hmm) with hmmbuild function from hmmer 3.2.1[78]. Gene prediction was performed at assembly level using prodigal 2.6.3[74] and parsed for matches using the built hmm model.

Linear correlation using Pearson correlation coefficient was calculated between *dsrB* and *hgcA* coverage, and between *mcrA* and *hgcA* coverage using python library pingouin[86].

Data availability

The data that support the findings of this study are openly available in the European Nucleotide Archive (ENA) with the reference number PRJEB58816 (https://www.ebi.ac.uk/ena/browser/view/PRJEB58816).

Received: 20 August 2024; Accepted: 5 February 2025
Published online: 28 February 2025

References

1. Shur, Y., Jorgenson, M. T., Kanevskiy, M. Z. & Permafrost. In *Encyclopedia of Snow, Ice and Glaciers* (eds Singh, V. P., Singh, P. & Haritashya, U. K.) 841–848 (Springer, 2011). https://doi.org/10.1007/978-90-481-2642-2_400
2. Schuster, P. F. et al. Permafrost stores a globally significant amount of mercury. *Geophys. Res. Lett.* **45**, 1463–1471 (2018).

3. Farbrot, H., Isaksen, K., Etzelmüller, B. & Gisnås, K. Ground thermal regime and permafrost distribution under a changing climate in Northern Norway. *Permafrost Periglac. Process.* **24**, 20–38 (2013).
4. Wu, R., Trubl, G., Taş, N. & Jansson, J. K. Permafrost as a potential pathogen reservoir. *One Earth*. **5**, 351–360 (2022).
5. Tarnocai, C. et al. Soil organic carbon pools in the northern circumpolar permafrost region. *Glob. Biogeochem. Cycles* **23**, (2009).
6. Miner, K. R. et al. Emergent biogeochemical risks from Arctic permafrost degradation. *Nat. Clim. Chang.* **11**, 809–819 (2021).
7. Natali, S. M. et al. Large loss of CO_2 in winter observed across the northern permafrost region. *Nat. Clim. Chang.* **9**, 852–857 (2019).
8. Poissant, L., Zhang, H. H., Canário, J. & Constant, P. Critical review of mercury fates and contamination in the arctic tundra ecosystem. *Sci. Total Environ.* **400**, 173–211 (2008).
9. Pavithra, K. G., SundarRajan, P., Kumar, P. S. & Rangasamy, G. Mercury sources, contaminations, mercury cycle, detection and treatment techniques: A review. *Chemosphere* **312**, 137314 (2023).
10. Harada, M. & Minamata disease: Methylmercury poisoning in Japan caused by environmental pollution. *Crit. Rev. Toxicol.* **25**, 1–24 (1995).
11. World Health Organization. Mercury and health. https://www.who.int/news-room/fact-sheets/detail/mercury-and-health
12. Selin, N. E. Global biogeochemical cycling of mercury: A review. *Annu. Rev. Environ. Resour.* **34**, 43–63 (2009).
13. Barkay, T. & Gu, B. Demethylation the other side of the mercury methylation coin: A critical review. *ACS Environ. Au*. **2**, 77–97 (2022).
14. Folhas, D. et al. Structural characterization of dissolved organic matter in permafrost peatland lakes. *Water (Switzerland)*. **12**, 1–18 (2020).
15. Deshpande, B. N., Macintyre, S., Matveev, A. & Vincent, W. F. Oxygen dynamics in permafrost thaw lakes: Anaerobic bioreactors in the Canadian subarctic. *Limnol. Oceanogr.* **60**, 1656–1670 (2015).
16. Parks, J. M. et al. The genetic basis for bacterial Mercury methylation. *Science* **339**, 1332–1335 (2013).
17. Compeau, G. & Bartha, R. Methylation and demethylation of Mercury under Controlled Redox, pH, and salinity conditions. *Appl. Environ. Microbiol.* **48** (1984).
18. Kerin, E. J. et al. Mercury methylation by dissimilatory iron-reducing bacteria. *Appl. Environ. Microbiol.* **72**, 7919–7921 (2006).
19. Hamelin, S., Amyot, M., Barkay, T., Wang, Y. & Planas, D. Methanogens: Principal methylators of mercury in lake periphyton. *Environ. Sci. Technol.* **45**, 7693–7700 (2011).
20. Bravo, A. & Cosio, C. Biotic formation of methylmercury: A bio–physico–chemical conundrum. *Limnol. Oceanogr.* **65** (2019).
21. Capo, E. et al. A consensus protocol for the recovery of mercury methylation genes from metagenomes. *Mol. Ecol. Resour.* **23**, 190–204 (2023).
22. Gilmour, C. C., Bullock, A. L., McBurney, A., Podar, M. & Elias, D. A. Robust mercury methylation across diverse methanogenic archaea. *mBio*. **9** (2): (2018). https://doi.org/10.1128/mBio.02403-17
23. Lin, H., Moody, E. R. R., Williams, T. A. & Moreau, J. W. On the origin and evolution of Microbial Mercury methylation. *Genome Biol. Evol.* **15**, evad051 (2023).
24. Peterson, B. D. et al. Metabolically diverse microorganisms mediate methylmercury formation under nitrate-reducing conditions in a dynamic hydroelectric reservoir. *ISME J.* **17**, 1705–1718 (2023).
25. Podar, M. et al. Global prevalence and distribution of genes and microorganisms involved in mercury methylation. *Sci Adv.***1** (9), e1500675 (2015). https://doi.org/10.1126/sciadv.1500675 (2015).
26. Barkay, T. & Gu, B. Demethylation-the other side of the mercury methylation coin: A critical review. *ACS Environ Au*. **2** (2), 77–97 (2021). https://doi.org/10.1021/acsenvironau.1c00022
27. Gionfriddo, C. M. et al. An improved hgcAB primer set and direct high-throughput sequencing expand Hg-Methylator diversity in Nature. *Front. Microbiol.* **11** (2020).
28. Laberge-Carignan, A. et al. Seasonal contrasts in dissolved Selenium Dynamics in Subarctic Thaw Lakes. *ACS Earth Space Chem.* **8** (2024).
29. Matveev, A., Laurion, I., Deshpande, B. N. & Bhiry, N. and W. F. Vincent. High methane emissions from thermokarst lakes in subarctic peatlands. *Limnol. Oceanogr.* **61** (2016).
30. Bhiry, N. et al. Environmental change in the Great Whale River region, Hudson Bay: Five decades of multidisciplinary research by Centre d'études nordiques (CEN). *Écoscience* **18** (2011).
31. Girard, C., Langlois, V., Vigneron, A. & Vincent, W. F. and A. I. Culley. Seasonal regime shift in the viral communities of a permafrost thaw lake. *Viruses* **12** (2020).
32. Vigneron, A., Cruaud, P., Bhiry, N. & Lovejoy, C. and W. F. Vincent. Microbial community structure and methane cycling potential along a thermokarst pond-peatland continuum. *Microorganisms* **7** (2019).
33. Vigneron, A., Lovejoy, C., Cruaud, P., Kalenitchenko, D. & Culley, A. and W. F. Vincent. Contrasting winter versus summer microbial communities and metabolic functions in a permafrost thaw lake. *Front. Microbiol.* **10** (2019).
34. Jonsson, S. et al. Arctic methylmercury cycling. *Sci. Total Environ.* **850**, 157445 (2022).
35. Gordon, J., Quinton, W., Branfireun, B. A. & Olefeldt, D. Mercury and methylmercury biogeochemistry in a thawing permafrost wetland complex, Northwest territories, Canada. *Hydrol. Process.* **30**, 3627–3638 (2016).
36. Loseto, L. L., Lean, D. R. S. & Siciliano, S. D. Snowmelt sources of methylmercury to high arctic ecosystems. *Environ. Sci. Technol.* **38**, 3004–3010 (2004).
37. Chen, C. F. et al. Dry and wet seasonal variation of total mercury, inorganic mercury, and methylmercury formation in estuary and harbor sediments. *J. Environ. Manag.* **253**, 109683 (2020).
38. Yu, R. Q., Reinfelder, J. R., Hines, M. E. & Barkay, T. Mercury methylation by the methanogen Methanospirillum hungatei. *Appl. Environ. Microbiol.* **79** (2013).
39. Baral, B. S. et al. Mercury binding by methanobactin from Methylocystis strain SB2. *J. Inorg. Biochem.* **141**, 161–169 (2014).
40. Lu, X. et al. Anaerobic Mercury methylation and demethylation by Geobacter bemidjiensis Bem. *Environ. Sci. Technol.* **50**, 4366–4373 (2016).
41. Darío, A. et al. Sulfate-reducing bacteria in floating macrophyte rhizospheres from an amazonian floodplain lake in bolivia and their association with hg methylation. *Appl. Environ. Microbiol.* **71**, 7531–7535 (2005).
42. Newsome, L. & Falagán, C. The microbiology of metal mine waste: Bioremediation applications and implications for planetary health. *GeoHealth* **5**, e2020GH000380 (2021).
43. Paape, T. et al. Adaptation to mercury stress by nitrogen-fixing bacteria is driven by horizontal gene transfer and enhanced gene expression of the mer operon. (2024). https://doi.org/10.21203/rs.3.rs-3854515/v1
44. Jong-In, H. et al. Complete genome sequence of the metabolically versatile plant growth-promoting Endophyte Variovorax paradoxus S110. *J. Bacteriol.* **193**, 1183–1190 (2011).
45. Oregaard, G. & Sørensen, S. J. High diversity of bacterial mercuric reductase genes from surface and sub-surface floodplain soil (Oak Ridge, USA). *ISME J.* **1**, 453–467 (2007).
46. Rincón-Tomás, B. et al. Revisiting the mercury cycle in marine sediments: A potential multifaceted role for Desulfobacterota. *J. Hazard. Mater.* **465**, 133120 (2024).
47. Grégoire, D. S. & Poulain, A. J. A physiological role for HgII during phototrophic growth. *Nat. Geosci.* **9**, 121–125 (2016).
48. Porwal, S. & Singh, R. Cloning of merA gene from methylotenera mobilis for mercury biotransformation. *Indian J. Microbiol.* **56**, 504–507 (2016).

49. Xu, R. et al. Metabolic potentials of members of the class Acidobacteriia in metal-contaminated soils revealed by metagenomic analysis. *Environ. Microbiol.* **24**, 803–818 (2022).
50. Arregui, G. et al. Mercury-tolerant Ensifer medicae strains display high mercuric reductase activity and a protective effect on nitrogen fixation in Medicago truncatula nodules under mercury stress. *Front. Plant Sci.* **11**, (2021).
51. Maxime, L. et al. Microbial diversity and mercury methylation activity in periphytic biofilms at a run-of-river hydroelectric dam and constructed wetlands. *mSphere* **6** https://doi.org/10.1128/msphere.00021-21 (2021).
52. Pierre Importance of Open Marine Waters to the Enrichment of Total Mercury and Monomethylmercury in Lichens in the Canadian High Arctic. *Environ. Sci. Technol.* **49**, 5930–5938 (2015).
53. Sharma, N., Wang, Z., Catalano, J. G. & Giammar, D. E. *Dynamic Responses of Trace Metal Bioaccessibility to Fluctuating Redox Conditions in Wetland Soils and Stream Sediments* (ACS Earth and Space Chemistry, 2022).
54. Chiasson-Gould, S. A., Blais, J. M. & Poulain, A. J. Dissolved organic matter kinetically controls mercury bioavailability to bacteria. *Environ. Sci. Technol.* **48** (2014).
55. Regnell, O. & Watras, C. J. Microbial Mercury methylation in aquatic environments: A critical review of published field and Laboratory studies. *Environ. Sci. Technol.* **53** (2019).
56. Gendron, A. & Allen, K. D. Overview of diverse methyl/alkyl-coenzyme M reductases and considerations for their potential heterologous expression. *Front. Microbiol.* **13** (2022).
57. Klier, K. M., Martin, C., Langwig, M. V. & Anantharaman, K. Evolutionary history and origins of dsr-mediated sulfur oxidation. *ISME J.* **18** (2024).
58. Jackson, T. A. The influence of clay minerals, oxides, and humic matter on the methylation and demethylation of mercury by micro-organisms in freshwater sediments. *Appl. Organomet. Chem.* **3**, 1–30 (1989).
59. Mehrotra, A. S. & Sedlak, D. L. Decrease in net Mercury methylation rates following Iron Amendment to Anoxic Wetland Sediment slurries. *Environ. Sci. Technol.* **39**, 2564–2570 (2005).
60. Zhang, L., Ren, F., Li, H., Cheng, D. & Sun, B. The influence mechanism of freeze-thaw on soil erosion: A review. Water (Switzerland) **13** (2021). https://doi.org/10.3390/w13081010
61. Varty, S., Lehnherr, I., Pierre, K., Kirk, J., Wisniewski, V. & st., & Methylmercury Transport and Fate shows strong seasonal and spatial variability along a high Arctic Freshwater Hydrologic Continuum. *Environ. Sci. Technol.* **55**, 331–340 (2021).
62. Barkay, T., Kroer, N. & Poulain, A. J. Some like it cold: Microbial transformations of mercury in polar regions. *Polar Res.* **30**, (2011).
63. Ma, M., Du, H. & Wang, D. Mercury methylation by anaerobic microorganisms: A review. *Crit. Rev. Environ. Sci. Technol.* **49**, 1893–1936 (2019).
64. Ri-Qing, Y., Tamar, B. & R, R. J., E, H. M. & Mercury methylation by the Methanogen Methanospirillum hungatei. *Appl. Environ. Microbiol.* **79**, 6325–6330 (2013).
65. United States Environmental Protection Agency (EPA). Method 1631, Revision E: Mercury in Water by Oxidation, Purge and Trap, and Cold Vapor Atomic Fluorescence Spectrometry. Washington, DC. (2002).
66. Hintelmann, H. & Ogrinc, N. Determination of stable mercury isotopes by ICP/MS and their application in environmental studies. In *Biogeochemistry of Environmentally Important Trace Elements, ACS Symposium Series*. American Chemical Society, pp. 321–3338. (2003). https://doi.org/10.1021/bk-2003-0835.ch021
67. United States Environmental Protection Agency (EPA). Method 1630: Methyl Mercury in Water by Distillation, Aqueous Ethylation, Purge and Trap, and Cold Vapor Atomic Fluorescence Spectrometry. Washington, DC. (1998).
68. Hintelmann, H., Jones, K. K. & Evans, R. D. Constants of mercury methylation and demethylation rates in sediments and comparison of tracer and ambient mercury availability. *Environ. Toxicol. Chem.* **19** (9), 2204–2214 (2000).
69. Hintelmann, H. & Evans, R. D. Application of stable isotopes in environmental tracer studies - measurement of monomethylmercury (CH3Hg+) by isotope dilution ICP-MS and detection of species transformation. *Fresenius J. Anal. Chem.* **358**, 378–385. https://doi.org/10.1007/s002160050433 (1997).
70. Christensen, G. A. et al. Development and validation of broad-range qualitative and clade-specific quantitative molecular probes for assessing mercury methylation in the environment. *Appl. Environ. Microbiol.* **82**, 6068–6078 (2016).
71. Jeon, S. A. et al. Comparison between MGI and Illumina sequencing platforms for whole genome sequencing. *Genes Genomics*. **43**, 713–724 (2021).
72. Chen, S., Zhou, Y., Chen, Y. & Gu, J. Fastp: An ultra-fast all-in-one FASTQ preprocessor. *Bioinf. Sep.* **1** (17), i884–i890. https://doi.org/10.1093/bioinformatics/bty560 (2018).
73. Li, D. et al. MEGAHIT v1.0: a fast and scalable metagenome assembler driven by advanced methodologies and community practices. *Methods* **102**, 3–11 (2016).
74. Hyatt, D. et al. Prodigal: Prokaryotic gene recognition and translation initiation site identification. *BMC Bioinform.* **11**, 119 (2010).
75. Langmead, B. & Salzberg, S. L. Fast gapped-read alignment with Bowtie 2. *Nat. Methods*. **9**, 357–359 (2012).
76. Li, H. et al. Genome Project Data Processing S: The sequence alignment/map format and SAMtools. *Bioinf. (Oxf. Engl.)*. **25**, 2078–2079 (2009).
77. Liao, Y., Smyth, G. K. & Shi, W. featureCounts: An efficient general purpose program for assigning sequence reads to genomic features. *Bioinformatics* **30**, 923–930 (2014).
78. Finn, R. D., Clements, J. & Eddy, S. R. HMMER web server: Interactive sequence similarity searching. *Nucleic Acids Res.* **39**, W29–W37 (2011).
79. Matsen, F. A., Kodner, R. B. & Armbrust, E. V. Pplacer: Linear time maximum-likelihood and bayesian phylogenetic placement of sequences onto a fixed reference tree. *BMC Bioinform.* **11**, 538 (2010).
80. RStudio Team. RStudio: Integrated Development for R. RStudio. https://posit.co/products/open-source/rstudio/
81. Menzel, P., Ng, K. L. & Krogh, A. Fast and sensitive taxonomic classification for metagenomics with Kaiju. *Nat. Commun.* **7**, 11257 (2016).
82. Christakis, C. A., Barkay, T. & Boyd, E. S. Expanded diversity and phylogeny of mer genes broadens Mercury Resistance paradigms and reveals an origin for MerA among Thermophilic Archaea. *Front. Microbiol.* **12**, (2021).
83. Edgar, R. C. MUSCLE: Multiple sequence alignment with high accuracy and high throughput. *Nucleic Acids Res.* **32** (2004).
84. Yang, S., Liebner, S., Alawi, M., Ebenhöh, O. & Wagner, D. Taxonomic database and cut-off value for processing mcrA gene 454 pyrosequencing data by MOTHUR. *J. Microbiol. Methods* **103** (2014).
85. Diao, M. et al. Global diversity and inferred ecophysiology of microorganisms with the potential for dissimilatory sulfate/sulfite reduction. *FEMS Microbiol. Rev.* **47** (2023).
86. Vallat, R. Pingouin: Statistics in Python. *J. Open. Source Softw.* **3** (2018).

Acknowledgements

This research was funded by Portuguese national funds through the Fundação para a Ciência e a Tecnologia (FCT) under the PERMAMERC project (PTDC/CTA-AMB/4744/2020) and the PhD grants to Beatriz Martins (2021.04818.BD) and Diogo Folhas Ferreira (SFRH/BD/145142/2019). Additional support was provided by FCT to the Centro de Química Estrutural, Instituto Superior Técnico (UIDB/00100/2020; UIDP/00100/2020) and the Interdisciplinary Centre of Marine and Environmental Research (UIDB/04565/2020; UIDP/04565/2020). This work also received support from the Portuguese Polar Program (PROPOLAR) and a "la Caixa" Foundation

fellowship to Nicola Gambardella (ID100010434; LCF/BQ/DI24/12070032).

Author contributions

Conceptualization (all authors); Data curation (CM, JC, NG); Formal Analysis (JC, NG, APR); Funding acquisition (CM and JC); Methodology (JC, NG, BM, DF); Resources (CM); Supervision (CM, JC); Writing - all authors; Review and editing (all authors).

Declarations

Competing interests

The authors declare no competing interests.

Additional information

Supplementary Information The online version contains supplementary material available at https://doi.org/10.1038/s41598-025-89438-7.

Correspondence and requests for materials should be addressed to C.M.

Reprints and permissions information is available at www.nature.com/reprints.

Publisher's note Springer Nature remains neutral with regard to jurisdictional claims in published maps and institutional affiliations.